3-DIMENSIONAL ANALYSIS OF ALVEOLAR CHANGES AFTER EXTRACTION AND IMPLANT PLACEMENT: A PILOT STUDY

Mark England Ludlow

A thesis submitted to the faculty of the University of North Carolina at Chapel Hill in partial fulfillment of the requirements for the degree of Master of Science in the School of Dentistry (Prosthodontics).

Chapel Hill
2015

Approved By:

Lyndon Cooper

Beatriz Paniagua

Ingeborg De Kok

ABSTRACT

Mark England Ludlow: 3-DIMENSIONAL ANALYSIS OF ALVEOLAR CHANGES AFTER EXTRACTION AND IMPLANT PLACEMENT: A PILOT STUDY
(Under the direction of Lyndon Cooper)

Objectives: The purpose of this study was to evaluate the dimensional change that occurs after tooth extraction and implant placement.

Materials and Methods: A protocol was developed for assessing the change in the buccal alveolar bone facial to the implants using the pre-operative and post-operative cone beam scans using three different software programs. DICOM files were formatted in 3D-Slicer, segmented further in ITK-SNAP, and aligned and measured in VAM.

Results: Eight patients' (4 grafted vs. 4 non-grafted) pre- and post-operative digital models were compared to assess linear alveolar change. The mean alveolar bone dimensional change facial to the implants at the crestal, mid-implant and apical regions was .974 ± .536 mm, .762 ± .371 mm, and .442 ± .259 mm respectively.

Conclusions: A protocol for comparing surface dimensional changes of alveolar bone was developed and used to compare clinical therapy outcomes.

TABLE OF CONTENTS

LIST OF FIGURES

Background

Tooth loss is a malady that effects nearly 70% of the individuals of the population of the United States (Bloom 1989). The most common causes of tooth loss include caries, periodontal disease, fracture, and trauma. The loss of a tooth leads to many and varied changes that occur within the alveolar process.

These changes were initially objectively studied in humans by Pietrokovski (1967). He used a split mouth comparison examining tooth bound uni-lateral edentulous ridges compared to normal dentate ridges. He noted that in the maxilla, buccal resporption was much more pronounced than palatal resorption with the center of the ridge shifting towards the palate. This result occurred in both arches and was more pronounced in the premolar and molar regions when compared to the anterior teeth.

Atwood observed similar resorption patterns when assessing fully edentulous participants (Atwood 1957). He contributed significantly to the timing of these events noting that a period of "measured bone loss" occurred immediately following full arch extraction. Tallgren further added to this concept by observing that this process of "rapid resorption" occurred "during the first year of denture wear" followed by a continuation of resorption over a twenty five year period at a slower rate (Tallgren 1972). Johnson continued to quantify these changes noting that the majority of the resorptive changes occurred during the first 10-24 weeks post extraction (Johnson 1969).

The biologic processes contributing to these changes were first observed and studied

in various animal models. Euler (1923), Claflin (1936), and Hubbel (1941) were among the first to note some of the changes in a dog model. They observed that a clot was generally formed first, followed by epithelial formation with bone formation and deposition occurring afterwards. Similar findings were observed in rats (Huebsch 1952), sheep (Harrison 1943), and monkeys (Raddon 1959).

From the fundamental principles gleaned from the animal research, Amler (1960, 1969) and colleagues began investigating this process in humans. They focused on the wound healing that occurred within the socket. They observed that nearly all sockets healed in a similar manner beginning with soft tissue closure. This occurred by the process of the formation of an immediate clot that was replaced with granulations tissue by the seventh day. This granulation tissue was then replaced by connective tissue by the twentieth day. From a bony perspective, bone formation was first noted at the bottom of the socket by the seventh day and filled at least two thirds of the socket by the thirty-fifth to the thirty-eighth day.

The issue of alveolar resorption following tooth extraction as related to subsequent dental implant placement was re-popularized in the late 1990's. Schropp et al (Schropp 2003) reported that, following single tooth extraction in humans, the alveolar bone remodeled rapidly. Within six months to one year, the alveolar width was significantly reduced. As described in their cross-sectional data, the buccal alveolar dimension was reduced by approximately 50%. The lingual bony plate was reduced to a lesser extent.

Cardaropoli furthered this research in an experimental study in dogs (Cardaropoli 2003). After the extraction of the distal root of mandibular premolars, he noted that a blood clot was formed in the socket during the first three days that was partially replaced by a

provisional matrix during the first seven days. By day fourteen, woven bone occupied nearly half of the socket which was mostly replaced by mineralized bone at thirty days. This was attributed to a peak in osteoblastic/osteoclastic activity during this time period (Trombelli 2008). Finally, bone marrow occupied the vast majority of the socket by the one hundred and eighty day mark.

Araujo and colleagues took a different approach to the healing alveolus and focused on the socket walls and the buccal and lingual plates (Araujo 2005). They noted that there was "marked osteoclastic activity" causing the resorption of the crestal bundle bone resulting in a significant vertical reduction of buccal and lingual height. Resorption then occurred from the "outer surfaces of both bony walls" creating the horizontal bone loss originally noted by Pietrokovski (1967), Atwood (1957), and others (Tallgren 1972). This also verified Johnson's(1969) work that demonstrated that the bone loss was greater in a horizontal direction than a vertical one.

In the canine model, the kinetic process of alveolar resorption was described (Araujo 2005). During an 8-week period, preferential buccal alveolar plate resorption occurred. This process was mediated by demonstrable osteoclastogenesis. It is also hypothesized that the preferential resorption of the buccal alveolar plate reflects the loss of the bundle bone that encompasses the Sharpey's fibers of the periodontal ligament oriented at the alveolar crest. Accordingly, tooth extraction and removal of Sharpey's fibers leads to irreversible loss of this crestal bone tissue. Notwithstanding, further resorption of the buccal alveolar plate has been recorded in longitudinal clinical studies (Vera 2012).

The overall dimensional changes occurring in the socket and in the buccal and lingual

plates were assessed and measured by Schropp (2003). Using clinical measurements on casts, subtractive radiography, and linear radiographic measurements, he assessed the post-extraction alveolar changes that occurred over a one-year period. From their clinical measurements, a reduction of the ridge width by 50% was observed over twelve months of which "two thirds occurred during the first three months of healing." During the first three months, an average of 1.2 mm in height was lost and one mm pocket reductions in the adjacent teeth were also observed.

Classifications

Because of the extreme changes that can occur within the alveolus after an extraction of a single tooth or multiple teeth, various ways to classify them have been developed. The first classification system was formulated by the works of Atwood in 1963. By using multiple series of cephalographs, a general pattern of boney resorption was noted and classified for the dentate to edentulous mandible. This classification contained 6 orders of changes with order number one being a dentate participant progressing through order number six which was a depressed residual ridge. Of note was a gross finding of the behavior of the buccal plate which "all but disappears in some specimens" further lending to our understanding of the rapid resorption of this alveolar structure.

This phenomenon was further classified and simplified by Seibert (1983). He defined ridge defects into three general categories. The least severe being a class I defect exhibiting a buccaolingual loss of tissue with normal height. A class II defect conversely showed no loss of buccolingual dimension, but had a marked apico-coronal loss. Where as class III defects were the most severe as they had both apico-coronal and buccolingual loss.

Allen (1985) further added to these classifications by assessing the depth of the defect relative to the adjacent ridge. A mild defect being less than 3mm. A moderate defect being 3-6mm in depth, and a severe defect being greater than 6mm.

Grafting

To overcome the apparent inescapable reality of alveolar resorption, clinicians have adopted different bone grafting approaches to maintain or regain buccal alveolar dimension following tooth extraction. Due to the rapid atrophy of the alveolus post-extraction as noted above, many researchers and clinicians were looking for ways to slow or stop the process by grafting different materials into the sockets (Lekovic 1997). They observed that grafting materials helped mitigate and avoid volume reductions and surface invaginations in sockets (Cardaropoli 2005). Grafts could also act as a scaffold for new bone formation (Cardaropoli 2005). These actions are thought to be brought about by three different mechanisms: osteogenisis, osteoinduction, and osteoconduction (Misch 1993). Osteogenesis is the process in which a material causes new bone to be developed and formed by osteoblasts. Osteoinduction is the process by which the substance stimulates osteogenisis by transforming mesenchyme cells into bone forming cells. Finally, an osteoconductive material provides a physical matrix or scaffold for bone deposition (Garg 2004).

These mechanisms of action are generally brought about by the physical composition of the materials of the graft themselves. Thus, some clinicians and researchers categorize the grafts according to this mode of action (Cardaropoli 2005). Others have classified grafts according to the source from which they are derived (Avila-Ortiz 2014). The three general types of bone grafting material are autogenous grafts, allografts, and Xenografts (Misch 1993). Each type can be used in different clinical situations depending upon the outcome

desired.

Autogenous Grafts

Autogenous bone has long been considered the gold standard for bone regeneration procedures (Nencovsky 1996) as it has been shown to have both osteogenic and osteoconductive properties (Burchardt 1983). This bone may be harvested from intra-oral sites including the mandibular symphysis and ramus, the maxillary tuberosity region, or exostoses. It may also be taken from extra-oral sites such as the tibia, the iliac crest, rib, or calvarium. While this has been commonly used for large graft procedures, the efficacy of using this type of graft in extraction sockets is questionable. In beagle dogs, Araujo (2010) placed autologous buccal bony chips in into fresh extraction sockets. After 3 months, the sites were measured and sectioned and he noted that "this type of graft material failed to prevent ridge contraction" as there was pronounced buccal bone resorption in both a vertical and horizontal direction as found in non-grafted areas (Araujo 2010). Conversely, with the use of a tenting screw and a bone marrow aspirate from the iliac crest, Pelegrine (2010) noted that this type of autogenous graft preserved the contraction of alveolar ridges.

Allograft

Allografts are a type of sterilized bone graft obtained from cadavers or from donors other than the participant (Garg 2004). Some benefits of this type of graft, verses autogenous bone grafts, are the lack of a secondary donor site thus leading to decreased surgery time, complications, and blood loss (Misch 1993). In general, these grafts are divided into two types: freeze-dried bone allograft (FDBA) and demineralized freeze-dried bone allograft (DFDBA). In general, these types of graft are thought to be ossteoconductive, but DFDBA

has also been shown to be osseoinductive due to the presence of various bone morphogenic proteins contained therein (Urist 1971). Iasella (2003) conducted a blinded randomized controlled trial comparing socket grafting with FDBA verses extraction socket alone and noted a significant decrease in buccal plate resorption with a difference in 1.6 mm between groups. They also noted a gain of vertical height of 1.3mm verses a loss of .9mm in the socket group. Fotek (2009) demonstrated even less dimensional changes by covering the FDBA grafts with either a polytetrafluoroethylene (PTFE) membrane or a dermal matrix. These additions limited the buccal resorption to .3 mm and .44 mm respectively compared to the preoperative assessment. Finally Borg (2014) compared FDBA vs. DFDBA in 42 human sockets and found no difference between the two relative to dimensional changes. He did however find that DFDBA produced significantly more vital bone (36.16% compared to 24.69%) and that it also had a lower mean percentage of residual graft (18.24% compared to 27.04%) (Borg 2014).

Xenografts

Xenografts are composed of tissue that is derived from one unlike species to another species. Generally, those most commonly used in humans are made of materials that are of porcine and of bovine derivation. These materials usually have a strictly ossteoconductive effect on the surrounding tissue but this has been debated (Artzi 2000). In an early study, Araujo (2008) observed that when grafting mongrel dogs with Bio-Oss, alveolar dimensional stability appeared to be attained, but that the process of healing in the extraction sites was dramatically slowed. In his later paper, he noted that only 12%, 4% and 4% of the alveolar process had contracted in the coronal, middle, and apical portions respectively compared to 35%, 3%, and 6% in the non-grafted sockets (Araujo 2009). Not only do xenografts appear

to maintain the shape of the alveolus better than non-grafted sockets, they also contain statistically greater volumes of bone and less connective tissue (Barone 2008).

Implants in bone

Due to the success of these various bone grafting modalities to assist in slowing the resorptive process of the alveolus after tooth extraction, other clinicians were wondering if placing an implant into these same sockets would yield similar results. From his study on the process of ridge atrophy in cadavers, Dennison (1993) recommended placing implants into fresh extraction sockets so as to mitigate the resorptive response. Watzek (1995) further added to this concept from his clinical study by recommending that implants be placed in serial extraction socket with the hope to preserve the buccal bone. Up to this point, no one had looked objectively at the clinical changes brought about by implant placement nor the histologic changes that were occurring. Thus, Paolantonio (2001) compared immediate implant placement into sockets verses implant placement into healed ridges. He concluded that there were no differences between the two groups and suggested that "early implantation may preserve the alveolar anatomy and that the placement of a fixture in a fresh extraction socket may help to maintain the bony crest structure". He also illustrated that the healed ridge and the extraction socket went through similar histologic changes.

These findings seem to be at odds with studies by other authors. Araujo (2005) and his group looked at the alveolar changes with their accompanying buccal and lingual wall changes that occurred with implant placement into immediate sockets in beagle dogs. They illustrated that even with the implant placement, the edentulous ridge showed "marked dimensional alterations" that were similar to those of ridges that had not received implant placement. They concluded that the placement of an implant into an extraction socket "failed

to prevent the re-modeling that occurred in the walls of the socket" due to a marked increase in osteoclastic activity (Araujo 2005).

Botticelli (2004) illustrated similar findings. Four months after implant placement upon re-entry into the extraction sites, they found that hard tissue had filled most of the bony gaps between the implant and the socket. Unfortunately, this new hard tissue deposition had failed to stop the reduction of the ridge as "56% of the horizontal buccal bone" was lost along with "30% of the palatal bone." Covani (2003) showed similar results showing a narrowing of the alveolus by 3.8mm post implant placement which tabulated to a 38% decrease in ridge dimension.

The vertical change that can occur with immediate implant placement is also a debatable subject. Some authors have found very little change to the magnitude of .8mm or less (Araujo 2006, Covani 2010). Araujo (2005) on the other hand found a vertical bone resorption of 2.6 mm after three months in a dog model.

Explaining the different results from these studies has proven difficult. One factor that has been shown to influence the amount of alveolar resorption has been the width of the residual socket. None of the previous authors cited examined this parameter. In a dog study by Qahash (2008), he specifically looked at the residual socket being a predictor for bony resorption. He demonstrated that when the buccal plate is less than 2mm in width, the buccal bone showed significantly higher rates (double the rate) of bone resorption. This width was also important "to maintain the alveolar bone at the implant platform" in a vertical direction. These suggestions are hard to translate to the human model as Huynh-Ba (2010) has demonstrated significantly thinner sockets in humans ranging from .8mm in the anterior

region to 1.1mm in the premolar area. To the point, that in his cohort of 93 participants, only 3% of the participants had a buccal plate 2mm or greater.

Facial Gap

Another possible factor that has been hypothesized to influence the dimensional changes in the alveolus is the gap that is between the fixture and the inner extraction socket wall. This gap frequently occurs with immediate placement as the socket is almost always of a larger diameter than the implant being placed. An early study by Harris (1983) examined implant placement for hip arthoplasty in dogs recommended a close fit between the implant and the bony site for proper osseointegration. This conclusion was based upon the observance of a lack of bone bridging a .5 mm gap between recipient site and implant. Carlsson's work (Carlsson 1988) in rabbits appeared to verify these findings. He noted that with gaps of .7 mm and 1.7 mm, some of the test animals continued to have residual gaps which were still present after twelve weeks of healing where as no gaps were present with intimate bone to implant contact at the time of placement.

Owing to this fact that some gaps were closed in Carlsson's study (1988). Botticelli (2003) conducted a similar experiment with dogs creating a 5mm deep and 1-1.125mm wide circumferential defect around the implants. At four months, complete resolution of the gap was achieved. In a later study (Botticelli 2004), he widened the gaps up to 3mm and observed that the gaps remained in only 8/52 subjects. Thus according to these studies, it appeared that in a healed ridge with an induced circumferential defect, bone could bridge a gap of up to 3mm from the socket to the implant.

Whether the bone could still bridge this gap in an extraction site was the next

question to be answered. Covani (2004) examined this process and found that in fresh extraction sockets, the bone could fill the gap without the use of membranes or grafting up to a gap size of 1.5mm. With defects larger than 1.5mm, the gaps were closed with connective tissue and not with direct bone to implant contact. Similar findings were observed in a study by Wilson (1998). He noted that gaps greater than 1.5 mm exhibited significantly reduced bone fill leading him to conclude that "the horizontal component of the peri-implant defect was the most critical factor relating to the final amount of bone-implant contact." Schropp echoed this (Schropp 2003), but found that even in defects of up to 5mm in width, 70% of the gap would be filled with bone spontaneously.

The timing of these events were evaluated by Araujo (2006). He showed that small defects of less than .3mm filled in after 4 weeks of healing. Conversely, larger defects (between 1-1.5 mm) were healed by 12 weeks post-op. Covani (2010) showed similar findings with nearly all gaps of 1mm filled at 4 weeks and completely filled at twelve weeks. These gaps were filled completely with a cortical bone layer adjacent to the implant with large marrow spaces occupying the rest of the area.

Other authors have questioned the capacity of the socket to heal spontaneously on its own and have recommended various grafting modalities. Boticelli (2003, 2004) compared placing barrier membranes over the implant and the gap to open sockets and found no difference in healing between the two. Covani (2004) illustrated similar results noting that open sockets and membrane covered sockets healed in a like manner. Araujo's group (Araujo 2010) carried out a split mouth design study in beagle dogs. In one site, they placed implants with Bio-Oss collagen filling the gap and compared it to their control group with no graft placement. They noted that this graft material decreased the rate of buccal resorption

better than their control group by providing an increased amount of hard tissue in the buccal wall. As already noted above, this was thought to be accomplished by a modification of healing and the delaying of the healing of the site (Araujo 2009).

Measurement and assessment of alveolar dimensional changes

The oldest method for assessing the changes noted above is by using standard measuring tools such as calipers (Pietrokovski 1967) , periodontal probes (Covani 2004), or other measuring devices. Covani (2004), for example, used a periodontal probe to measure the width of the alveolus by laying the probe flat while centering it through the implant. This technique can have its limitations as the perception of the measurement could be changed by the angle of the observer to the probe. Another technique, employed by Lekovic (1997), involved fixation of a bone screw to the mid-facial area of the alveolus and using multiple measurements from this area with a probe. This technique, while creating a fixed landmark, also has limitations mostly brought about by the limitations of the human eye. It is generally regarded that the accuracy of a measurement range can only be reliably detected as low as .3mm by the naked eye. One final technique of note that tried to correct this problem by moving away from the periodontal probe was that employed by Casado (2010). After tooth extraction, an acrylic stent was placed over the surgical site and holes made in the buccal and lingual and the ridge width was measured via calipers. This stent was then re-adapted later and similar measurements were taken. While for general measurements, these methods are useful to determine two-dimensional changes on flat objects, they have their limitation for reliably assessing three-dimensional changes.

Radiography is another tool that has been used to try to quantify bony alveolar

changes. However, Lang and colleagues (Lang 1977) demonstrated that conventional radiographic assessment has been of limited value for the detection of subtle bony changes and has often been associated with the under-estimation of these changes. Moreover, Rudolph illustrated that even a .85 mm bony change could not be visualized with conventional radiography (Rudolph 1987). Because of these limitations, other techniques were developed including digital subtraction radiography introduced in the early 1980's (Gronhdahl 1983). This technique uses conventional radiographs taken at different time points utilizing uniform position, settings, contrast, and densities (Christgau 1998). These radiographs are then combined causing the unchanged areas to be subtracted and the areas of change appearing either darker or lighter in the image. Christgau (1998) demonstrated that this technique was able to detect minute bony changes of approximately 200 microns for cortical bone and 500 microns for trabecular bone. Thus, he concluded that digital subtraction radiography demonstrated an accurate "quantitative assessment of subtle changes in the alveolar bone." It is for this reason, that many of the studies looking at bony alveolar changes have used this modality to quantify these changes. Unfortunately, this technique was relegated to two dimensional, planar radiography.

As good as this technique is in quantifying these subtle minute bony changes, it still has further limitations. Differences in positions or orientations at the time of x-ray exposure can lead to discrepancies on the digitally subtracted images. Rudolph noted that even a one-degree angulation change between radiographic pairs led to noise, artifacts, and image degradation (Rudolph 1987). He further demonstrated that with a two to three degree angulation change, a change in the thickness of the cortical bone of .35 mm was only detectable 50% of the time and .42 mm was able to be detected most of the time. While this

specificity of detection is significantly better than conventional radiography (Rudolph 1987), it still has the limitations of quantifying three-dimensional bony changes in a two-dimensional manner.

Another approach for evaluating and quantifying these alveolar changes has come about with the advent and use of cone beam computed tomography (CBCT). This has grown in popularity and use due to the ability to image 3-dimensional structures with relatively low radiation doses and short scan times when compared to medical grade computed tomography (Agbaje 2007). Lund explored the accuracy of measurements taken from CBCT of metal samples of know sizes with acrylic beads embedded in them (Lund 2009). The difference between the real and CBCT measurements was between .08 to .09mm which was significantly smaller than the voxel size of .125mm. He concluded, "linear measurements derived from CBCT was highly accurate". Timock furthered this work by applying it to human structures. He measured the height changes and thickness changes in the alveolus (Timock 2011). When comparing the measurements in the same areas with digital calipers, the CBCT measurements "did not differ significantly from direct measurements and there was no pattern of underestimation or overestimation." The mean differences were .3mm in the buccal bone height and .13 mm in the buccal bone thickness.

This modality has also been shown to be accurate when assessing the bone around dental implants. Shiratori placed implants into eight cadaver maxillas and was able to compare the accuracy of the CBCT measurements to the measurements derived from an optical microscope of the physical skull (Shiratori 2012). He found no significant difference between the two measuring modalities and attained only a 2% mean difference between them and concluded that "CBCT can be considered a precise method for measuring the buccal

bone volume around dental implants."

The difficulty in assessing bony changes over time is that computed tomography volumes must be attained at different periods of time. These volumes must then be able to be compared to one to another to accurately assess the changes that can occur. This assessment can only take place if the virtual models rendered from the computed tomography data accurately represent the physical conditions in the alveolus. Damstra evaluated the accuracy of these models by comparing them to physical models of cadaver mandibles embedded with multiple glass beads (Damstra 2010). They observed that the measurement differences between the two models were between .0 - .16 mm and that the differences weren't statistically significant.

Baumgaertel took a slightly different approach to verifying accuracy (Baumgaertel 2009). He assessed clinical measurements such as overbite, overjet, intermolar and intercanine width, and arch length to verify positional accuracy and model accuracy of the CBCT rendered models. No significant difference was noted for the two measurement modalities although taking all measurements as a composite, a significant difference was noted in that the CBCT rendered models slightly underestimated the size of the physical model.

The final note on accuracy is how well do CBCT generated models compare to the gold standard of medical grade CT (MSCT) rendered models. Liang measured this exact issue relative to physical skulls scanned with a high-resolution optical scanner (Liang 2010). The mean deviation for MSCT was .137 mm verses between .165 and .386 mm for various CBCT systems. All differences were significant, but very small differences were obtained

which “do not necessarily have clinical significance.”

Materials and Methods

From a previous prospective randomized controlled trial (IRB #11-1057), eighteen participants were recruited from the participant pool at the dental school and graduate prosthodontics program and accomplished treatment. To be included in the study, the participants had to meet the following criteria:

- Have a tooth #5-12 requiring extraction
- Have natural teeth adjacent to the proposed site
- Be at least 18 years of age
- Available for one-year follow-up
- Consent to the trial.

The participants followed a clinical protocol consisting of the following:

- Initial exams and records including pre-operative CBCT scan
- Extraction of the hopeless tooth.
- Random assignment into a group (group one receiving no graft and group two receiving a large particle Bio-Oss graft in the facial gap).
- Implant placement to proper depth and healing abutment placement.
- Screw retained provisionalization three-months after implant placement
- Definitive cement retained restorations after seven months.
- Post op records including follow up CBCT scans were achieved after ten

months.

Upon the gathering of records and data following the study, only eight pre-operative and post-operative scans were able to be used out of the eighteen participants. The problems with the records were grouped as follows:

- 1 file type was corrupted
- 1 follow up scan was of the wrong area
- 6 scans were formatted in a way rendering them incompatible with the software that was being used in the study. This could also have been an exporting problem with the scans.
- 2 post-operative scans were missing

The eight remaining pairs of CBCT data were then de-identified and assigned numerical identifiers.

Slicer Segmentation

All scans were then opened in Slicer version 4.3 (Cambridge, MA) and were converted from dicom file types to nearly raw raster data (nrrd) file types. This file type is used to support scientific visualization and medical image processing as it can accurately convey N-Dimensional raster (dot-matrix computer graphics) information (Aja-Fernandez 2009). This helps to convey spacial orientations and directions of the scanned object (www.slicer.org). All files were then renamed and saved in a separate folder. The nrrd files were then opened again with Slicer 4.3 in order to segment the files according to intensity. A slicer extension called "Intensity Segmenter" was downloaded and integrated into Slicer 4.3.

This tool segments the nrrd files according to the intensity value of the corresponding structures within the image volume. This segmentation is accomplished by using the Hounsfield radiodensity scale to define the different tissue densities through out the scan. This scale sets the radiodensity of water at zero and ranges from air being roughly -1000 HU to cortical bone being upwards of 3000 HU. According to Kirkos and Misch (Misch 1999), the Hounsfield units for the different densities of bone involved in implant placement are as follows:

D1 bone: >1250 Hounsfield units
D2 bone: 850 to 1250 Hounsfield units
D3 bone: 350-850 Hounsfield units
D4 bone: 150 to 350 Hounsfield units

After perusing multiple scans and measuring the Hounsfield units of various alveolar cortical plates, it was decided that 400 HU would be our starting point for the segmentation as this showed to be the most accurate starting place for segmenting. A text document range file was created to be used in the intensity segmenter program. The base document had the following values:

-infty 400 0
400 +infty 1

This document is then used by the Slicer extension to create a colored label over anything that is greater than 400 HU in density. This is accomplished by opening Slicer 4.3 and selecting the Intensity Segmenter extension. The input image is selected from the nrrd file that we are using. In the output label image drop down, "create and rename volume" is selected and the file name is changed to reflect that this will be a segmentation image. The

range file is then selected and the file is run to segment the volume. (Figure 1)

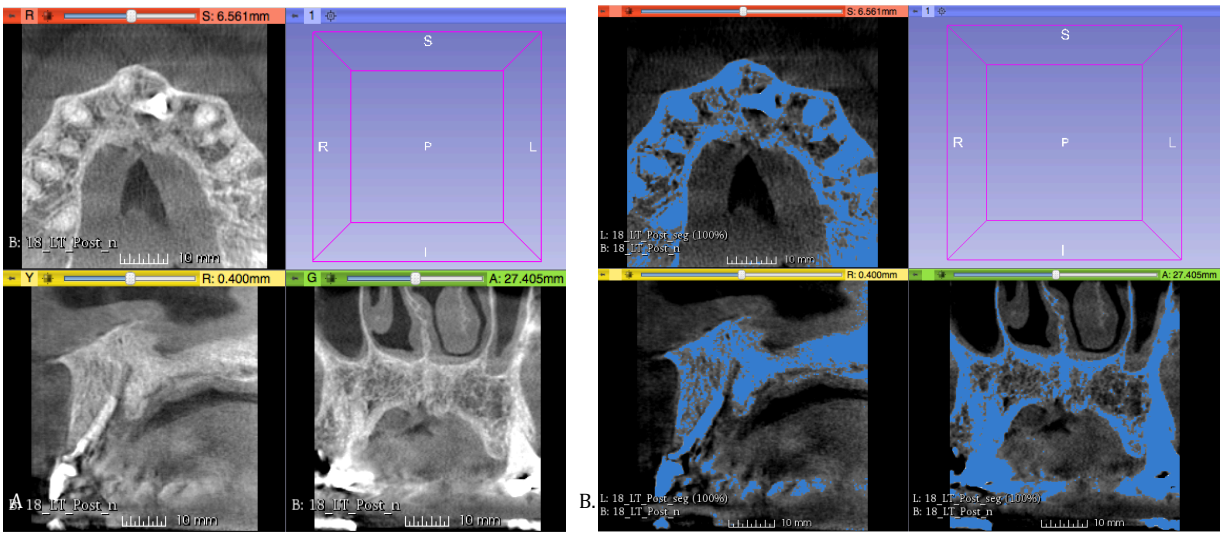

Figure 1. A) Represents the pre-segmented image when loaded into 3D-Slicer. B) Represents the results of the auto-segmentation by the Intensity Segmenter module of 3D-Slicer.

Three other density range text documents were created decreasing the Hounsfield units to 350, 300, and 250 respectively. These were used in cases where the bone density of the scan was lower than our standard 400 and more segmentation needed to be taken place (Figure 2). Each volume was then inspected so as to assure the greatest bone segmentation with the least amount of segmentation errors (such as segmenting tissue as bone, etc). All pre-operative and post-operative scans were run through this process. Initial attempts to match the Hounsfield units of the pre-operative and post-operative scans proved unsuccessful as each scan volume was taken at slightly different settings or in a slightly different orientation which caused the structural densities to differ between pairs. The segmentations were matched manually between pre- and post-operative pairs to the best of our ability by using the different range files for each one. All the segmentation files were then saved as nrrd files.

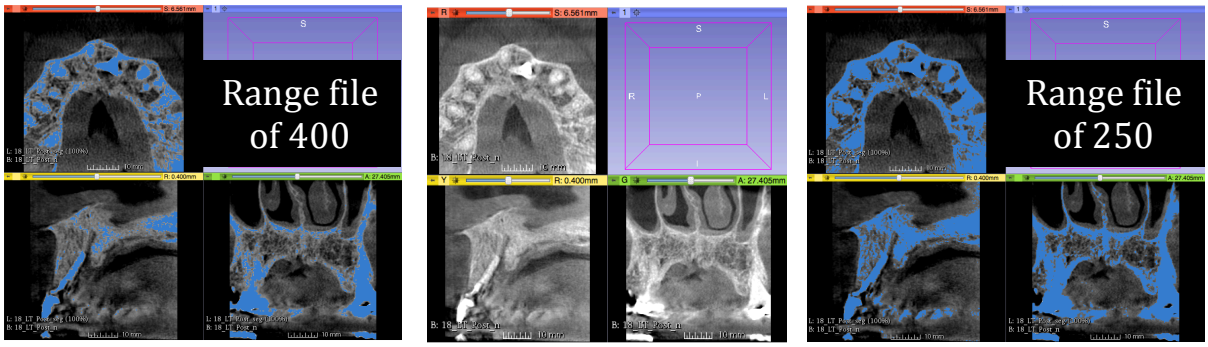

Figure 2. These pictures illustrate the different segmentations that can occur with the use of different range files of varying Hounsfield units. The non-segmented image is in the center with the file on the left being segmented with a range file set at 400 HU. Conversely, the file on the right is segmented at 250 HU. It is noted that the buccal alveolar bone is more readily observed in the segmentation of the range file of 250 HU.

ITK-Snap segmentation

ITK-Snap version 3.2.0 was used to next open the original nrrd volume files as gray scale images. Subsequently, the segmentation images were then loaded and overlaid on the gray scale images (original nrrd file) as a colored overlay upon the base image. This color highlighted representation of the segmentation was named "label 1". Full 3-dimensional models were then rendered in ITK-Snap of the entire segmented scan. The label 1 covering the mandible was then removed via the scalpel tool by making the "active label" a clear label and drawing over all labels. The mesh was then updated reflecting the change, thus providing a model representing the maxilla and region of interest. On the scans where the scatter from the teeth or the occlusion of the teeth precluded a clean mandibular segmentation, the segmentation slice cuts were made as close as possible by approximation of scatter or opposing teeth without removing any of the maxillary teeth.

At this point, the image contrast was changed on all scans to best visualize the cortical bone on the maxillary arch. To aid in visualizing the cortical bone plate, five curve

control points were selected along the 3 most distal points being nearly at the top of the output image intensity (Figure 3). The mid-point approximated 400 HU, but more closely matched the value from the range file used previously. The terminal point was set at zero.

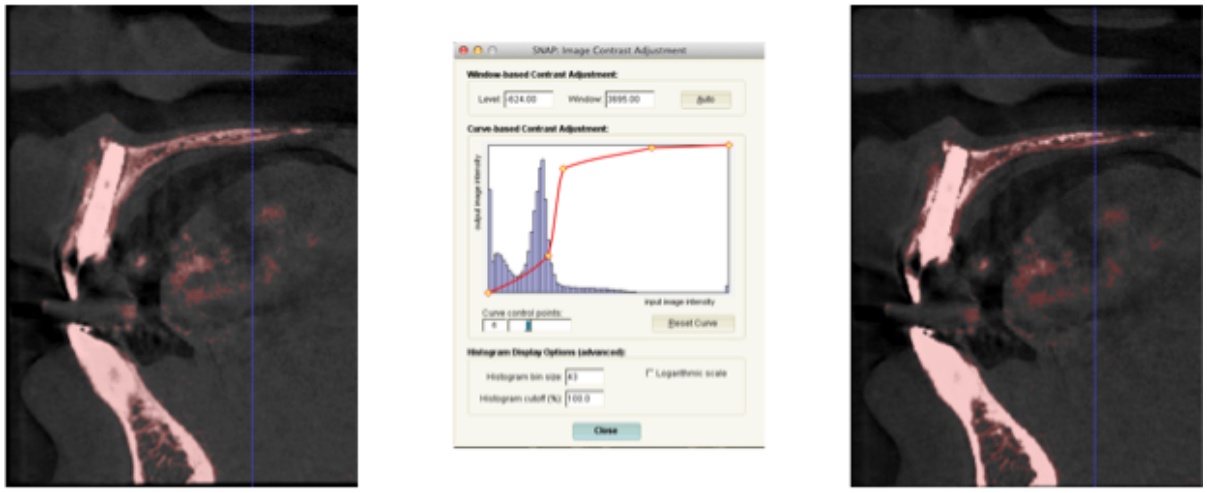

Figure 3. By adjusting the histogram (figure in the center) subtle differences in density are more easily observed. The figure on the left is pre-adjusted and it is somewhat difficult to visualize the bony plate facial to the middle/apex of the implant. In the figure on the right, the histogram has been adjusted and it is easier to distinguish the bony plate.

Using this established histogram, the volumes were then further segmented with the auto-segmentation tools in ITK-Snap. The snake tool was the principle means of further segmentation. This type of segmentation is based upon either the edges of the input image or the regions of uniform intensity (www.itk-snap.org) within the image. Label 1 was selected to be the "active label" and the program was configured to draw over the clear label. This step is needed to enable ITK-Snap to fill in the areas that the previous segmentation in Slicer could not accurately mark. The label 1opacity was decreased, enabling visualization of the bone through the label to verify the accuracy of the segmentation. The snake tool icon is then activated.

The selection box was then made to fit the region of interest for segmentation in all

three planes. The first step of segmentation in ITK-Snap, Segment 3-D was selected and the "intensity regions mode" of segmentation was used. The preprocessed image was chosen with the smoothness increased to a maximum value. The upper threshold was maintained to what the program recommended, but the lower threshold was adjusted to minimize noise and artifact labeling. This number differed for each scan and was even dissimilar within participants' pre- and post-operative scans. The second step involved the use of "spherical snake initialization bubbles", tools to enable segmentation in a defined sphere, by placing them in areas within the cortical plates where the labels still were not marking the bone. Care was taken to change the dimension of the bubbles so as to not place these outside the cortical housing of the alveolus. A third step of snake segmentation is required. Here, the parameters were a balloon force of 1.0 and a curvature force of 0.65 which would render a relatively smooth surface. The snake controller was run multiple times to optimize the representation of the alveolus and to minimize observed artifacts. This was visually verified by constantly updating the mesh so as to illustrate the 3-D mesh surface that was being formed. When an artifact and representative alveolar surface was accomplished, the auto-segmentation was finalized (Figure 4).

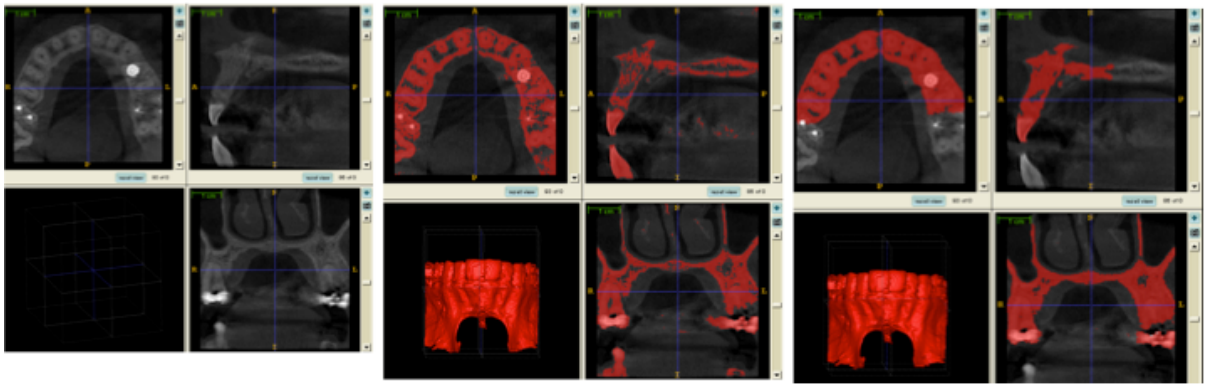

Figure 4. This figure represents the full process of automatic segmentation via ITK-Snap. The figure on the left represents the pre-segmented .nrrd file. The figure in the middle represents the results of the 3D-Slicer segmentation process. Whereas the figure on the right, represents the full automatically segmented file via ITK-Snap

These 'automatically' segmented images required further manual segmentation to assure the fidelity of the 3-D mesh. This was accomplished by the paint segmentation tool (Figure 5). A round paintbrush was selected using the 3-D brush option. The size of the brush varied according to the area that needed attention. The volume was visually inspected and Label 1 was either added or removed according to the accuracy of the auto-segmentation. Particular attention was paid to buccal plates in the area of the implant placement and the adjacent teeth. The teeth were manually segmented to the best of the operator's ability and the gross scatter and artifacts were removed. Once the manual segmentation was finished, an updated 3-D model surface mesh was rendered and a screenshot was taken of the image. This image was used as a template for the matching scan pair (pre- to post-operative or vice versa). All images were cleaned and segmented using the same tools and workflow and were saved as segmentation images and the surface meshes of each model were exported in the STL format. At the completion of this step (segmentation), each participant's pre-operative and post-operative CBCT images were available as segmented STL files for comparison.

Figure 5. After automatic segmentation via ITK-Snap is accomplished, the file is then further segmented by hand via the paintbrush tool (illustrated above).

Surface to surface rendering

Pre- and post-operative .STL surface meshes were then opened in VAM® v. 3.7.6 (Canfield Scientific Inc., Fairfield, NJ). This program is used to perform surface-to-surface registration and also to calculate measurements between specific points on each surface mesh. Both meshes were moved bodily in space until similar 3-dimensional orientations were visually confirmed. The surface-to-surface registration module was activated and the post-operative image was selected to match the pre-operative image. Full surface matching was selected. Where possible, the images provided sufficient common data points to enable automatic registration (Figure 6). In cases were significant data heterogeneity was present, pre- and post-operative images were registered by manual assistance. This process required the selection of 10 – 12 analogous surface points on both surface meshes (Figure 7). VAM

calculated successful registrations in this alternative manner. Quality of fit was verified visually.

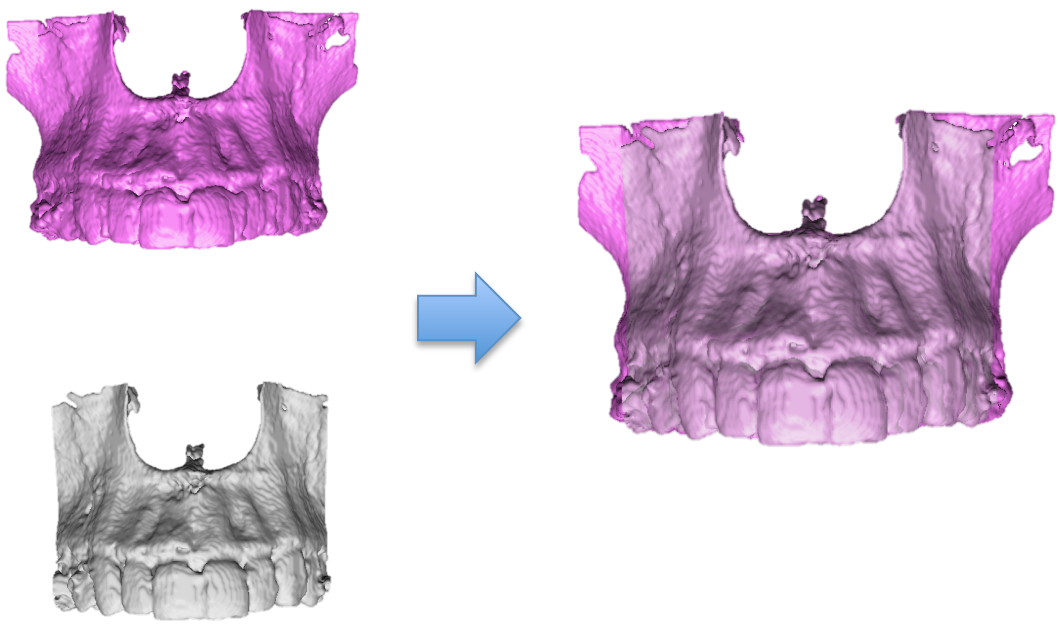

Figure 6. This represents the process of automatic surface registration via VAM software (Canfield Scientific). The pre-operative and post-operative surface meshes have enough common data points to allow the software to merge the two meshes together.

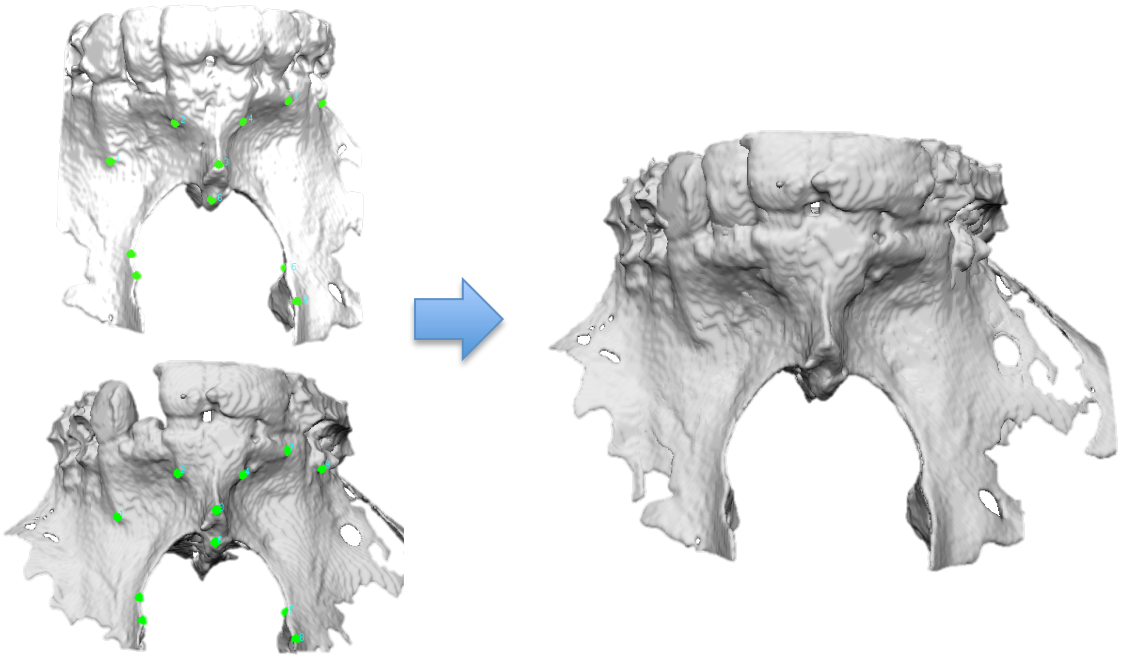

Figure 7. For surface meshes that displayed too much heterogeneity in the surfaces, manual registration was accomplished. Ten to twelve points easily identifiable points were selected on the both the pre- and post-operative surface meshes. The VAM (Canfield Scientific) software then meshed these points together rendering a fully registered pre- and post-operative model.

The registered surface meshes now permitted measurement and comparison. Registration landmarks were removed and greater emphasis was directed to the implant region of interest. To initiate measurement of the alveolar dimension facial to the implant, three landmarks were placed on the buccal bone surface specifically oriented to a) the crest region of the implant, b) the midpoint of the implant and c) the apex of the implant (Figure 8). Care was taken to assure that the markers were lined up accurately on the pre- and post-op meshes and markers were replaced were any deviation was noted.

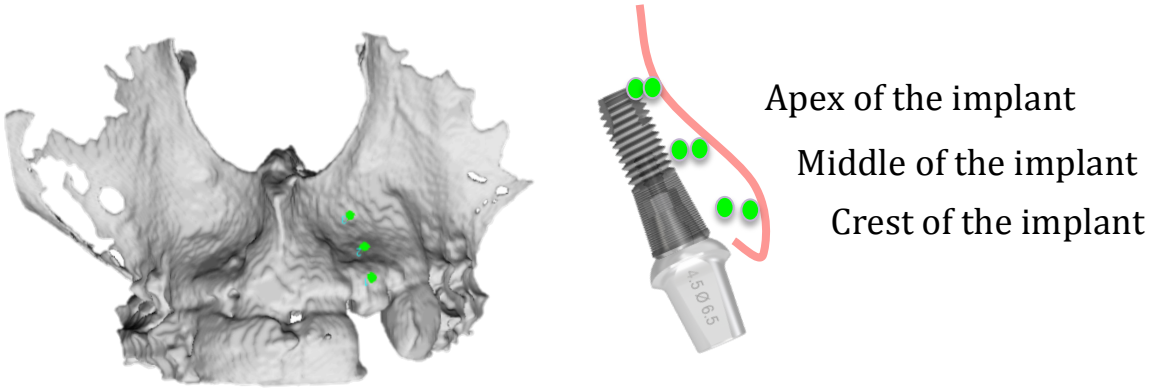

Figure 8. This figure illustrates the process of landmark placement for measuring in the VAM (Canfield Scientific). Three points were chosen at the apex, middle, and crest of the implant on both the pre-operative and post-operative surface meshes and the distance between the two points were calculated.

To assure consistency and to help decrease any human error or biases due to surface registration, all pairs were surface registered three times and measurements were taken all three times. Measurements were made at the same points along the buccal wall for the crestal, mid, and apex measurements. These areas were defined by evaluating where the implant was from the cross-sectional scan and correlating it with the root structures/alveolar landmarks in the surface rendering. Furthermore, the surface defects or landmarks were also used to consistently measure the three points in roughly the same areas when measuring after a new surface merge was accomplished. The correlated and modified surface meshes were then saved in .obj format so as to retain their spacial orientations to one another.

Statistical Analysis

Mean values for crestal, mid-implant and apical measures of buccal bone dimension were calculated in SPSS. Non-grafted and grafted groups were also compared via a T-test due to normal distribution of the data.

Results

Under an IRB approved protocol, 18 participants' pre and post-operative CBCT images related to maxillary anterior dental implant therapy were obtained. The DICOM files were extracted and evaluated. Of the 18 identified participants, three participants lacked either a pre- or post-operative CBCT images. Of the remaining 16 participants, six images had been archived as digital files incompatible with further analysis (not DICOM), and one additional participant's pre-operative file was corrupted. Eight intact and useful DICOM pairs were available for investigation within the identified and approved patient cohort.

Measurement of the alveolar bone facial to the single implant revealed alveolar bone facial to all implants and along all implant surfaces. Regarding implants in the non-grafted participant group, the mean alveolar bone dimension facial to implants at the crestal, mid implant and apical regions was 1.07 ± .638 mm, .845 ± .383 mm, and .480 ± .191 mm respectively. For the grafted participant group, the mean alveolar bone dimension facial to implants at the crestal, mid implant and apical regions was .876 ± .415mm, .670 ± .348 mm, and .404 ± .318mm respectively (P=.378) (Figure 9).

Mean bony change	Std. Deviation	Graft	No graft	Sig
.44243 mm	.25907 mm	.40445 mm	.48042 mm	.378
.76227 mm	.37054 mm	.66990 mm	.85463 mm	.230
.97460 mm	.53555 mm	.87584 mm	1.07333 mm	.485

Figure 9. Results of the statistical analysis by SPSS. The dashed line represents the pre-operative bony position and the solid line represents the final position of the buccal crest. All changes are noted in the table.

A workflow (Figure 10) was established to enable volumetric comparisons of the pre- and post-operative surface images related to the alveolar bone adjacent to single tooth implants. The workflow consisted of: 1) DICOM file conversion to nnrd files using Slicer, 2) automated nnrd segmentation in Slicer, 3) automated and manual refinement of segmentation in ITK-Snap, and conversion to and exportation of related .STL files, 4) surface registration of surface meshes in VAM, and 5) measurements

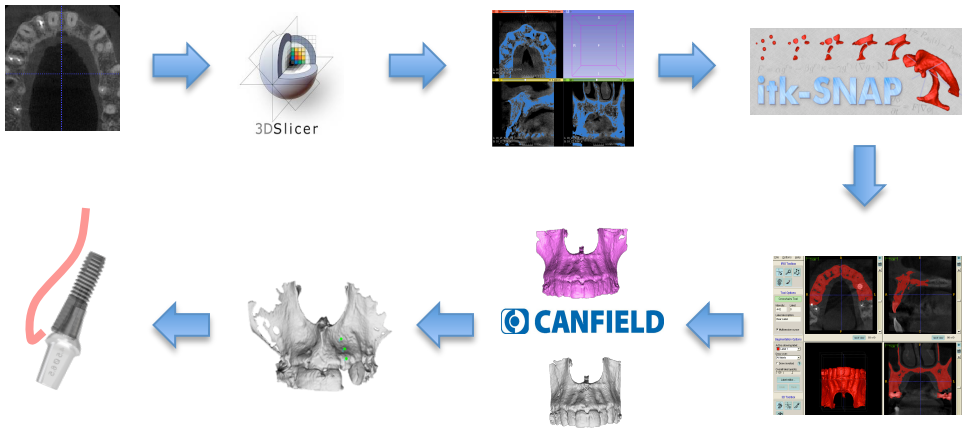

Figure 10. Represents all of the steps required in the workflow of analyzing linear alveolar changes from DICOM images.

Discussion

A primary goal of this project was to define a workflow for the volumetric longitudinal comparison of alveolar bone facial to dental implants. There were various hurdles that were encountered while developing this protocol to analyze and measure the changes that were occurring at the alveolus after extraction and implant placement. They can be broken down into five different areas which each had its own challenge and issue. They are categorized as:

- Problems with the original scans
- Auto-segmentation challenges in Slicer
- Challenges with ITK-Snap segmentation
- Difficulties with surface registration
- Consistency and accuracy of measurements

Problems with the original scans

Many of the difficulties that were encountered as we progressed through this project had their genesis in the original scan volumes taken pre-operatively and post-operatively. The original project called for the use of CBCT scans from two other clinical trials run at the University of North Carolina School of Dentistry. After locating 40 scans and converting them all to .nrrd files an unsurpassable problem was encountered. When these files were loaded into ITK-Snap the image volumes became undiagnostic around the implant fixture and the adjacent buccal plate. Areas that should have been exhibiting a very high radiopaque value were showing large areas of black surrounding the implant and other similarly dense areas. This is due to a phenomenon commonly known as “wrap around.” All of the CBCT

scans taken by the Galileos unit were internally programmed to code the densities to a certain scale. The difficulty lies in that the ITK-Snap software functioned with a smaller scale so all of the radiopaque densities above the ITK-Snap scale were then taken to the beginning of the scale and thus registered as radiolucent thus rendering the areas that should be radiopaque as radiolucent. This made it impossible to use the 40 scans from that study and an additional 20 from another study.

Another factor that rendered the scans useless in the study was how some of them were exported and saved. With the current cohort of participants, six of their scans were exported and saved as slices (Figure 11) instead of as complete volumes. The original volumes were changed to slices and it was impossible to stitch all of the slices together to create a full 3-dimensional model. Due to this six out of the eighteen participants were excluded from the project.

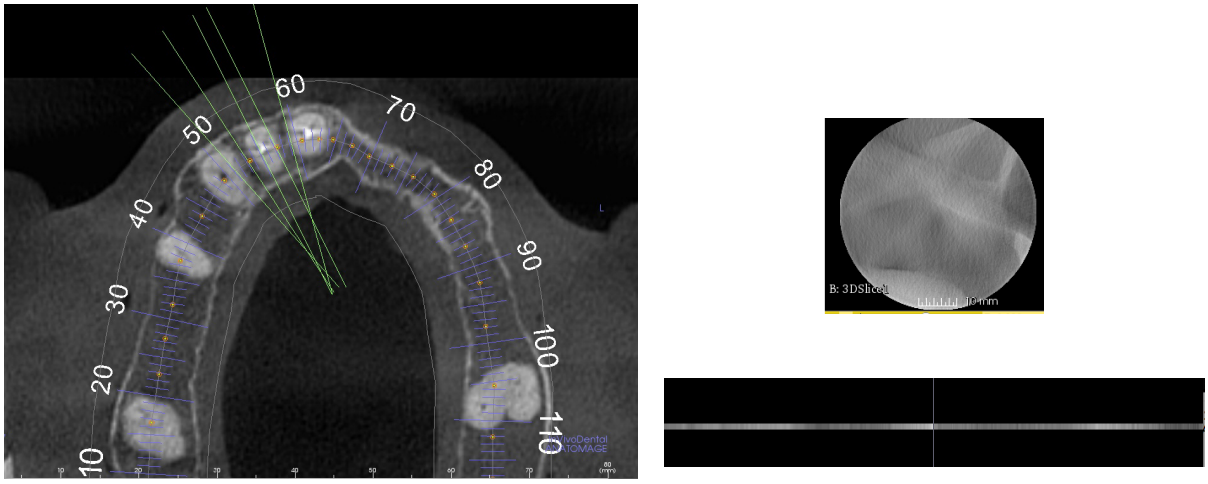

Figure 11. Illustrated a major hurdle with the study. The figure on the left is indicative of a full volume of information derived from a CBCT scan. The image on the right is illustrative of the files that were exported as slices. This difference led to the exclusion of 6 patients.

An additional potential challenge was encountered with the way in which the scans were exported. In order to consolidate space, each large field of view scan is exported with a

.3 mm voxel but the scan is actually taken with .16 mm voxel. Owing to the fact that the final resolution can only be as good as its voxel size, this smaller voxel size may have enabled an even greater ability to measure the changes occurring at the buccal plate. Damstra (2010) illustrated a similar finding by decreasing voxel size from .40 mm to .25 mm, but the overall measurement differences were statistically insignificant. However, it would still be recommended for future projects using similar protocols to export the scans with the smallest voxel size available.

The final difficulties that were experienced with the scans were the inconsistency of positioning and settings (Figure 12). Many participants were scanned with completely different positions and fields of view from pre-operative to post-operative scans. This led to a variety of problems in the scans ranging from important structures being cut off in the final volumes to an increase in the scatter and noise. A participant specific bite jig could be used so as to position the participant the same way in each subsequent scans. The "scout mode" could also be used so as to evaluate positioning prior to the taking of the full scan.

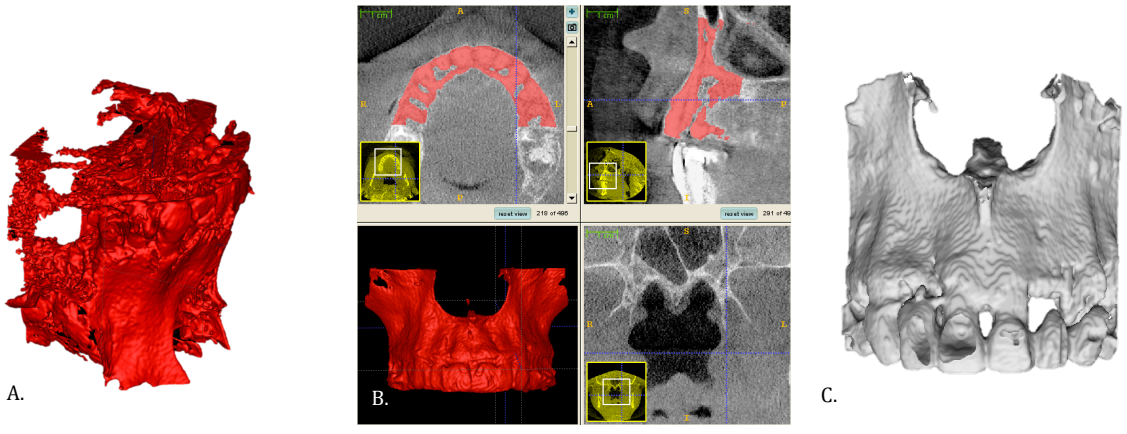

Figure 12. This figure is representative of many of the problems encountered with the scan images that were acquired. A) Represents a scan whose settings are less than optimal for the patient thus creating scatter through out the entire scan. B) Is indicative of a similar problem as A. This scan has too much noise in the soft tissue due to a settings problem. C) Illustrates problems with positioning. The anterior teeth of #'s 7,8 were cut off due to improper positioning.

Auto-segmentation in Slicer

The biggest challenge that was encountered in the segmentation of the images with the Slicer software had to do with the complete segmentation of the buccal alveolar plate of the maxilla. Owing to the fact that neither the settings nor the participant positions were consistent from the pre-operative to the post-operative scans, the buccal plate was never of a similar Hounsfield value. As noted above, 400 HU worked for the vast majority of the scans but needed to be decreased for a good portion of them. Also, two of the scans were taken with a different unit and this further impacted the difficulty in standardizing the HU's.

Challenges with ITK-Snap segmentation

Developing the protocol was the most difficult in this stage of the project. After the images were preliminarily segmented and a preliminary masked model was made, our initial attempts to segment the model were very subjective and nearly all by hand. The volume was cropped to show the implant site and only the two to three adjacent teeth. The snake segmentation was accomplished but then the entire volume was manually segmented by hand from the 3 cross sectional windows. The resulting 3-dimensional surface mesh was completely unsmooth and inaccurate (Figure 13) even though it appeared completely accurate from the cross sectional views. This was likely due to the difficulty visualizing thin tissues by CBCT. Mol (2008) demonstrated that the ability to diagnose minute bony changes in the anterior maxilla was very difficult owing

to the thinning and tapering of the alveolus at the crest. It was for this reason, that the initial protocol was changed to allow the software to segment out the buccal bone with minimal subjective input from the investigator.

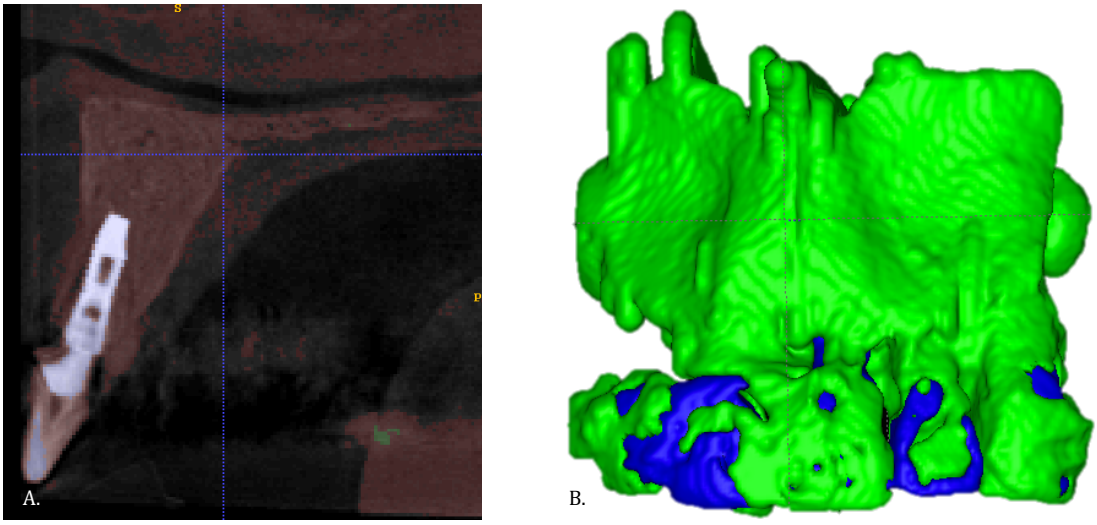

Figure 13. This image further illustrates difficulties with segmentation. A) Represents problems distinguishing very thin bone in the anterior crest. B) Represents initial attempts at segmentation with it's accompanying non-smooth surface mesh.

The second challenge was of a similar vein. With the snake auto-segmentation, once the settings were established to enable segmentation of the buccal plate, it was challenging to define the extent to which the automation proceeded. Auto-segmentation will occur indefinitely unless the operator intervenes in a step-wise manner. Manual control of this endpoint resulted in consistent representation of the buccal alveolar bone without risk of underrepresentation or noise. While subjective in nature, other reasonable alternatives were not apparent. As mentioned above, the acquisition of DICOM data with more similar settings, more reproducible positioning and consistent instrumentation would have eliminated much of this manual adaptation in segmentation.

Surface registration

The challenge of surface registration may be related to the difficulties in creation of segmented images and the resultant surface meshes. Dissimilar images precluded automatic surface-to-surface registration. Fifty percent of the meshes did not automatically register and were registered by point registration. While the evaluator estimated the registrations to be of sufficient quality, it may be argued that the complicating features of scatter throughout dental restorations of teeth could create variability in the integrity (goodness of fit) of the registration step.

Consistency and accuracy of measurements

After all the surface meshes were registered, the measurement steps presented a few challenges. The first was the ability to precisely visualize where the implant was. Unlike planning software, the surface meshes are not transparent nor are other cross sectional views available in VAM. While to goal of the study was to measure the changes in the buccal surface of the alveolar bone, the project was limited by the absence of information regarding the implant position. The implant was alternatively visible within the ITK-Snap window. Thus, the location of crestal, mid-implant and apical measuring points relative to the implant in the vertical dimension was only extrapolated to the VAM image. Further, these measurement points required duplication within paired pre- and post-operative images. Another source of error could be the marker placement on subsequent merges. Every attempt was made to place them in a reproducible manner, but this limitation is noted. Additional

effort to control this variable should be explored. However, measurements between examples varied by only a magnitude of .2 to .3mm, which is a very small number considering the exported voxel size was only .3mm.

Conclusions

A workflow for volumetric assessment of alveolar bone changes at dental implants involving assessment of pre and post operative CBCT images was developed. Three different software programs were required to create superimposed images that were sufficiently segmented and accurately superimposed to permit measurement. When pre- and post-operative images were compared, the difference in position of the buccal alveolar bone was reduced in magnitude ranging from .974 mm to .442 mm. The method used was associated with an error of approximately 0.3 mm or similar to the acquired image voxel size. In this small sample size, no significant difference was observed in buccal bone positional changes for immediate implants with or without alveolar grafting. Further advances in software to efficiently permit comparison of alveolar bone changes following clinical implant therapy is warranted.

REFERENCES

Bloom B, Gaft HC, Jack SS. National Center for Health Statistics. Dental services and oral health. United States, 1989. Vital Health Stat 10 (183). DHHS Pat No (PAS) 93-1511.

Pietrokovski, J Massler, M. Alveolar ridge resorption following tooth extraction. J Pros Dent January 1967 Vol 17 No 1.

Atwood DA. A cephalometic study of the clinical rest position of the mandible. Part II. The variability in the rate of bone loss following the removal of occlusal contacts. J Pros Dent 7; 1957, 544-552.

Tallgren, A. The continuing reduction of the residual alveolar ridges in complete denture wearers: a mixed longitudinal study covering 25 years. J Pros Dent 27; 1972 120-132

Johnson K. A study of the dimensional changes occurring in the maxilla following tooth extraction. Australian Dental Journal 1969; 14: 241-244

Euler, H. Die Heilung von Extraktionswunden, Deutsche Monatschr. Zahn 41:685; 1923

Claflin, R. S Healing of Disturbed and Undistrubed Extraction Wounds. J Am. Dent A 1936, 23: 945.

Hubbell, A. O.: Extraction Wounds and Therapeutic Agents: an Experimental Study, J. Am. Dent A 1941,28;251

Huebsch, R. F., Coleman, R. D., Frandson,M. M. and Recks, H: The Healing Process Following Molar Extractions, Oral Surg, Oral Med. And Oral Path. 5: 864. 1952

Harrison, J; Healing of Routine and of Severely Traumatized Exodontic Wounds. Burr 1943; 43: 107.

Raddon H; Local Factors in Healing of the Alveolar Tissues, Ann Roy Coll Surg England 1959; 24: 366.

Amler, M Johnson, P Salman, I. Histological and histochemical investigation of human alveolar socket healing in undisturbed extraction wounds. J Am Dent Assoc 1960;61:46–48.

Amler, M The time sequence of tissue regeneration in human extraction wounds. Oral Surg, Oral Med, and Oral Path 27;3 1969 309-318

Cardaropoli G, Araujo M, Lindhe J; Dynamics of bone tissue formation in tooth extraction sites. An experimental study in dogs. J Clin Periodontal 2003; 30, 809-818

Trombelli L, Farina R, Marzola A, Bozzi L, Liljenberg B, Lindhe J. Modeling and remodeling of human extraction sockets. J Clin Periodontal 2008; 35: 630-639

Araujo MG, Lindhe J: Dimensional ridge alterations following tooth extraction. An experimental study in the dog. J Clin Periodontal 2005; 32: 212-218

Vera, C DeKok, I Chen, W Reside, G Tyndall D, Cooper L. Evaluation of post-implant buccal bone resporption using cone beam computed tomorgraphy: A clinical pilot study. IJOMI 2012; 27; 1249-1257

Schropp L, Wenzel A, Kostopoulos L, Marring T. Bone healing and soft tissue contour changes following single-tooth extraction: A clinical and radiographic 12-month prospective study. Int J of Perio and Rest Dentistry 26; 2003 313-323

Atwood DA; Postextraction changes in the Adult Mandible as Illustrated by Microradiographs of Midsagittal sections and serial Cephalometric Roentgenograms; J Pros Dent 13;5 1963 810-824

Seibert, JS. Reconstruction of Deformed, Partially Edentulous Ridges, Using Full Thickness Onlay Grafts. Part I. Technique and Wound Healing. Compendium Vol 4; 5 1983 437-453

Allen EP, Gainza CS, Farthing GG, Newbold DA. Improved technique for localized ridge augmentation. J Perodontology April, 1985; 195-199

Lekovic V, Kenney EB, Weinlaender M, Han T, Klokkevold P, Nedic M, Orsini M. A bone regenerative approach to alveolar ridge maintenance following tooth extraction. Report of 10 cases. J Clin Periodontol 1997;68:563–570

Cardaropoli G, Araujo M, Hayacibara R, Sukekava F, Lindhe J. Healing of extraction sockets and surgically produced-augmented and non-augmented-defects in the alveolar ridge. An experimental study in the dog. J Clin periodontal 32:2005 435-440

Misch CE, Dietsh F. Bone-grafting materials in implant dentistry. Implant Dent 1993;2: 158–167

Garg AK. Bone Biology, Harvesting, and Grafting for Dental Implants. 2004 Quintessence publishing. Pgs 69-149

Avila-Ortiz G, Elangovan S, Kramer KWO, Blanchette D, Dawson DV. Effect of Alveolar Ridge Preservation after Tooth Extraction: A systematic review and meta-analysis. J Dent Res (2014) 93 (10): 950-958

Nencovsky CE, Serfaty V. Alveolar ridge preservation following extraction of maxillary anterior teeth. Report on 23 consecutive cases. J Periodontol (1996): 67:390-395

Burchardt H. The biology of bone graft repair. Clin Orthopaedics and Rel Res 1983; 174;April; 28-42

Araujo MG, Lindhe J. Socket grafting with the use of autologous bone: an experimental study in the dog. Clin Orl Impl Res, 2010; 1-5

Pelegrine AA, Sorgi da Costa CE, Correa ME, Marques JF. Clinical and histomorphometric evaluation of extraction sockets treated with an autologous bone marrow graft. Clin Oral Impl Res. 21, 2010, 535-542

Garg, A. Bone Biology, Harvesting, and Grafting for dental implants: rationale and clinical applications. 2004. ISBN- 0-86715-441-1

Urist MR, Strates BS Bone morphogenic protein. J Dent Res 1971 Nov-Dec;50(6):1392-1406.

Iasella JM, Greenwell H, Miller RL, Hill M, Drisko C, Bohra A, Scheetz JP Ridge preservation with freeze-dried bone allograft and a collagen membrane compared to extraction alone for implant site development: A clinical and histological trial in humans. J Periodont 2003; 74:7; 990-999

Fotek PD, Neiva RF, Want HL. Comparison of dermal matrix and polytetrafluoroethylene membranes for socket bone augmentations: A clinical and histologic study. J of Periodontol 2009, 80; 776-785

Borg TD, Mealey BL. Histologic healing following tooth extraction with ridge preservation using mineralized freeze dried bone allograft alone verse a combined mineralized-demineralized freeze dried bone allograft. A randomized controlled clinical trial. J of Periodontol 2014

Artzi Z, Haim T, Dayan D. Porous bovine bone mineral in healing of human extraction sockets. Part 1: Histomorphometric evaluations at 9 months. J Periodontol 2000:71:1015-1023

Araujo MG, Linder E. Wennstron J. Lindhe J. The influence of Bio-Oss collagen on healing of an extraction socket: an experimental study in the dog. The Int J of Per Res Dent 28; 2008; 123-135

Araujo MG, Lindhe J. Ridge preservation with the use of Bio-Oss collagen: A 6 month study in the dog. Clin Oral Impl Res 20, 2009; 433-440.

Barone A, Aldini N, Fini M, Giardino R, Guirado J, Covani U. Xenograft verses extraction alone for ridge preservation after tooth removal. A clinical and histomorphometric study. J Periodontol 2008; 79:1370-1377.

Dennisen HW, Kalk W, Veldhuis HAH, Van Waas MAJ. Anatomic considerations for preventive implantation. IJOMI 1993; 8;191-196

Watzek G, Haider R, Mensdorf-Pouilly N, Haas R. Immediate and delayed implantation for compete restoration of the jaw following etraction of all residual teeth: A retrospective study comparing different types of serial immediate implantion. IJOMI 1995: 10:561-567

Paolantonio M, Dolci M, Scarano A, D'Archivio D, Placido G, Tumini V, Piattelli A. Immediate implantation in fresh extraction sockets. A controlled clinical and histological study in man. J Periodontol 2001; 72;1560-1571

Araujo MG, Sukekava F, Wennstrom JL, Lindhe J. Ridge alterations following implant placement in fresh extraction sockets; an experimental study in the dog. J Clin Periodontol 2005; 32: 645-652

Botticelli D, Berglundh T, Lindhe J. Hard tissue alterations following immediate implant placement in extraction sites. J Clin Periodontol 2004; 31: 820-828

Covani U, Cornelini R, Barone A. Bucco-lingual bone remodeling around implants placed into immediate extraction sockets: A case series. J Periodntol 2003;74:268-273

Araujo MG, Sukekava F, Wennstrom JL, Lindhe J. Tissue modeling following implant placement in fresh extraction sockets Clin Oral Implants Res 2006:17:615-624

Covani U, Cornelini R, Calvo JL, Tonelli P, Barone A. Bone Remodeling around implants placed in fresh extraction sockets. Int J Period Rest Dent 2010; 30: 3-9

Qahash M, Susin C, Polimeni G, Hall J, Wikesjo U. Bone healing dynamics at buccal peri-implant sites. Clin Oral Impl Res 2008;19; 166-172

Huyhn-Ba G, Pjetursson B, Sanz M, Cecchinato D, Ferrus J, Lindhe J, Lang N. Analysis of the socket bone wall dimensions in the upper maxilla in relation to immediate implant placement. Clin. Oral Impl Res 2010;22; 37-42

Harris WJ, White RE, McCarthy JC, Walker PS, Weinberg EH. Bony ingrowth fixation of the acetabular component in canine hip joint arthroplasty. Clin Orth and Rel Res 1983; 176:7-11

Carlsson L, Rostlund T, Albrektsson B, Albrektsson T. Implant fixation improved by close fit. Acta Ortho Scand 1988;59:272-275

Botticelli D, Berghlundh T, Buser D, Lindhe J. The jumping distance revisited. Clin Oral Impl Res 2003; 14; 35-42

Botticelli D, Burglundh T, Lindhe J. Resolution of bone defects of varying dimension and configuration in the marginal portion of the peri-impant bone. An experimental study in the dog. J Clin Periodontol 2004; 31: 309-317

Covani U, Bortolaia C, Barone A, Sbordone L. Bucco-lingual crestal bone changes after immediate and delayed implant placement. J Periodontol 2004; 75:1605-1612

Wilson T, Schenk R, Buser D, Cochran D. Implants placed in immediate extraction sites: a report of histologic and histometric analyses of human biopsies. IJOMI 1998; 13:333-341

Schropp L, Kostopoulos L, Wenzel A. Bone healing following immediate versus delayed placement of titanium implants into extraction sockets: A prospective clinical study. IJOMI 2003; 18:189-199

Araujo M, Wennstrom J, Lindhe J. Modeling of the buccal and lingual bone walls of fresh extraction sites following implant installation. Clin Oral Impl Res 2006:17:606-614

Covani U, Cornelini R, Calvo JL, Tonelli P, Barone A. Bone remodeling around implants placed in fresh extraction sockets. Int J Perio Rest Dent 2010;30: 3-9

Araujo MG, Linder E, Lindhe J. Bio-Oss collagen in the buccal gap at immediate implants: a 6-month study in the dog. Clin Oral Impl Res 2010:10:1-8

Lekovic V, Kenney EB, Weinlaender M, Han T, Klokkevold P, Nedic M, Orsini M. A bone regernative approach to alveolar ridge maintenance following tooth extraction. Report of 10 cases. J Periodontol 1997:68:563-570

Casado PL, Duarte ME, Carvalho W, da Silva LE, Barboza EP. Ridge bone maintenance in human after extraction. Implant Dent 2010; 314-322

Lang NP, Hill RW. Radiographs in periodontics. J Clin Perio 1977;4;16-28

Grondahl HG, Grondahl K, Webber RL. A digital subtraction technique for dental radiography. Oral Surg Oral Med oral Path 1983;55;96-102

Christgau M, Hiller, KA, Schmalz G, Kolbeck C, Wenzel A. Quantitative digital subtraction radiography for the determination of small changes in bone thickness. Oral Surg Oral Med Oral Path Oral Rad 1998;85:462-472

Rudolph DJ, White SC, Mankovich NJ. Influence of geometric distortion and exposure parameters on sensitivity of digital subtraction radiography. Oral Surg Oral med Oral Path 1987; 64:631-637

Agbaje JO, Jacobes R, Maes F, Michiels K, Steenberghe D. Volumetric analysis of extraction sockets using cone beam computed tomography: a pilot study on ex vivo jaw bone. J Clin Periodontol 2007; 34; 985-990

Lund H, Grondahl K, Grondahl HG. Accuracy and precision of linear measurements in cone beam tomography Accuitomo tomograms obtained with different reconstruction techniques. Dentomaxillofacial Radiology 2009; 38:379-386

Timock AM Cook V McDonald T Leo MC Crowe J Benninger BL Covell D. Accuracy and reliability of buccal bone height and thickness measurements from cone-beam computed tomography imaging. Am J Orthod Dentofacial Orthop 2011; 140:734-744

Shiratori LN, Marotti J, Yamanouchi J, Chilvarquer I, Contin I, Tortamano-Neto P. Measurement of buccal bone volume of dental implants by means of cone-beam computed tomography. Clin Oral Impl Res 2012;23: 797-804

Damstra J, Fourie Z, Slater J, Ren Y. Accuracy of linear measurements from cone-beam computed tomography-derived surface models of different voxel sizes. Am J Orthod Dentofacial Orthop 2010:137:16e1-e6.

Baumgaertel S, Palomo JM, Palomo L, Hans M. Reliability and accuracy of cone-beam computed tomography dental measurements. Am J Orthod Dentofacial Orthop 2009; 136:19-28

Liang X, Lambrichts I, Sun Y, Denis K, Hassan B, Li L, Pauwels R, Jacobs R. A comparative evaluation of Cone Beam Computed Tomography (CBCT) and Mutli-Slice CT (MSCT). Part II: On 3D model accuracy. Eur J of Radio 2010; 75: 270-274

Aja-Fernández, Santiago; de Luis Garcia, Rodrigo; Tao, Dacheng; Li, Xuelong (2009). *Tensors in Image Processing and Computer Vision*. Advances in Computer Vision and Pattern Recognition. Springer Science & Business Media

Misch C. *Contemporary implant dentistry*, ed2, St Louis, 1999, Mosby

Mol A, Balasundaram A. In vitro cone beam compute tomography imaging of periodontal bone. Dentomaxillofacial Radiology 2008; 37: 319-324.